

Diboson anomaly: heavy Higgs resonance and QCD vector-like exotics

D. Aristizabal Sierra*

IFPA, Dep. AGO, Université de Liège, Bat B5, Sart-Tilman B-4000 Liège 1, Belgium.

J. Herrero-Garcia†

Department of Theoretical Physics, School of Engineering Sciences, KTH Royal Institute of Technology, AlbaNova University Center, 106 91 Stockholm, Sweden

D. Restrepo‡

Instituto de Física, Universidad de Antioquia, A.A. 1226, Medellín, Colombia.

A. Vicente§

Instituto de Física Corpuscular (CSIC-Universitat de València), Apdo. 22085, E-46071 Valencia, Spain.

The ATLAS collaboration (and also CMS) has recently reported an excess over Standard Model expectations for gauge boson pair production in the invariant mass region $1.8 - 2.2$ TeV. In the light of these results, we argue that such signal might be the first manifestation of the production and further decay of a heavy CP-even Higgs resulting from a type-I Two Higgs Doublet Model. We demonstrate that in the presence of colored vector-like fermions, its gluon fusion production cross-section is strongly enhanced, with the enhancement depending on the color representation of the new fermion states. Our findings show that barring the color triplet case, any QCD “exotic” representation can fit the ATLAS result in fairly large portions of the parameter space. We have found that if the diboson excess is confirmed and this mechanism is indeed responsible for it, then the LHC Run-2 should find: (i) a CP-odd scalar with mass below ~ 2.3 TeV, (ii) new colored states with masses below ~ 2 TeV, (iii) no statistically significant diboson events in the $W^\pm Z$ channel, (iv) events in the triboson channels $W^\pm W^\mp Z$ and ZZZ with invariant mass amounting to the mass of the CP-odd scalar.

I. INTRODUCTION

The ATLAS collaboration has recently reported an excess over the Standard Model (SM) expectations for gauge boson pair production in the invariant mass region of $1.8 - 2.2$ TeV [1]. The statistical significance of the excess observed by ATLAS is 3.4σ , 2.6σ and 2.9σ in the WZ , WW and ZZ channels, respectively, although the hadronic nature of the search makes it hard to distinguish gauge bosons implying some overlap between these channels. The CMS collaboration has also reported some moderate excesses in diboson searches both in hadronic channels [2] and in semileptonic channels [3], again at invariant masses around 2.0 TeV. Although the statistical significance is lower in this case ($1 - 2\sigma$), the fact that these excesses occur at roughly the same invariant mass value has made the *diboson excess* a hot subject in the community.

Although further data from the LHC Run-2 is required to confirm a diboson overproduction at $1.8 - 2.2$ TeV, it is tempting to speculate about new physics scenarios where these hints would be naturally explained. The obvious explanation to the ATLAS and CMS hints is a bosonic resonance that decays into a pair of SM gauge bosons.

In order to be able to explain the LHC data, the hypothetical candidate must face two requirements [1] (see also [4–6] for general analyses of the ATLAS data): (i) it has to be produced with a relatively high cross-section in the $\sim 1 - 10$ fb ballpark, and (ii) it should be a narrow resonance (with $\Gamma \lesssim 200$ GeV) decaying dominantly to a diboson final state. Many candidates with these properties have been already proposed¹. Although most references focus on spin-1 candidates, such as W'/Z' states in extended gauge models [4, 11–41], other alternatives are perfectly viable. Examples of such alternatives are spin-2 states [42] and triboson production [43]. Finally, spin-0 particles are among the simplest candidates to explain the diboson excess and have been considered in [34, 42, 44–53].

In this paper we propose the heavy Higgs (H) of a type-I Two Higgs Doublet Model (2HDM) as the resonance behind the diboson excess. Its production cross-section at the LHC is dominated by the standard gluon fusion process, strongly enhanced by the presence of new vector-like (VL) colored fermions. Furthermore, a large production cross-section for the heavy Higgs naturally implies negligible VL contributions to the gluon fusion cross-section for the light Higgs (h), which remains SM-

* daristizabal@ulg.ac.be

† juhg@kth.se

‡ restrepo@udea.edu.co

§ avelino.vicente@ific.uv.es

¹ Other recent works related to the diboson excess include an effective theory approach to the anomaly [7] and implications on dark matter searches [8], grand unification [9] or neutrinoless double beta decay and lepton flavor violation [10].

like. Once produced, the heavy Higgs decays to WW and ZZ final states, leading to the diboson excesses found by ATLAS and CMS. Regarding the VL states responsible for the heavy Higgs production, **we consider several $SU(3)_c$ representations: 3, 6, 8, 10 and 15**. QCD exotics (non-triplet $SU(3)_c$ representations) are well motivated in this context due to their large contributions to the gluon fusion cross-section [54].

Another model with an extended scalar sector and VL colored states has been put forward as an explanation to the diboson excess in [53]. Our setup differs from the one considered in this reference in several aspects. First, in our case the heavy Higgs resonance is embedded in a 2HDM framework which constrains its couplings and decay modes. Second, we go beyond the fundamental representation and explore the phenomenology induced by higher $SU(3)_c$ multiplets. In fact, we will show that a heavy scalar produced in gluon fusion driven by $SU(3)_c$ triplets cannot account for the diboson excess. One needs the enhancement coming from a larger color factor in order to achieve production cross-sections of the required size. Finally, we will also comment on some technical differences in the phenomenological analysis.

The rest of the manuscript is organized as follows. In sec. II, we discuss the features of extra VL colored fermions, the structure of the scalar sector, the colored VL fermions mass matrices and the relevant couplings. In sec. III, we study the phenomenological aspects of our scenario, in particular we discuss the different relevant aspects of the heavy Higgs production cross-section: group theory factors, α_S RGE running and VL fermion mass limits. In sec. III C, we present our main findings. Finally, in sec. IV we present our conclusions.

II. VECTOR-LIKE COLORED FERMIONS

The setup we consider involves extra VL colored fermions (n_{VL} VL generations) with the following $(SU(3)_c, SU(2)_L)_{U(1)_Y}$ transformation properties:

$$\begin{aligned} Q_L &= (d_R, \mathbf{2})_{\frac{1}{6}}, & Q_R &= (d_R, \mathbf{2})_{\frac{1}{6}}, \\ U_L &= (d_R, \mathbf{1})_{\frac{2}{3}}, & U_R &= (d_R, \mathbf{1})_{\frac{2}{3}}, \\ D_L &= (d_R, \mathbf{1})_{-\frac{1}{3}}, & D_R &= (d_R, \mathbf{1})_{-\frac{1}{3}}, \end{aligned} \quad (1)$$

where $d_R = \mathbf{3}, \mathbf{6}, \mathbf{8}, \mathbf{10}$ and $\mathbf{15}$. We decompose the $SU(2)_L$ doublets as

$$Q_{L,R} = \begin{pmatrix} \tilde{U} \\ \tilde{D} \end{pmatrix}_{L,R}, \quad (2)$$

such that $Q(\tilde{U}) = 2/3$ and $Q(\tilde{D}) = -1/3$. In addition to these states and the usual SM fermions, the scalar sector involves two hypercharge +1 scalar electroweak doublets, H_1 and H_2 .

The resulting 2HDM must of course yield a scalar with SM-like properties, something that in the absence of the

VL states is readily achievable by moving towards the decoupling limit [55]. However, in the presence of the new VL colored states this condition is not sufficient: the couplings to the VL states can potentially modify the SM Higgs production cross-section. Thus, in order to guarantee phenomenological consistency we endow our setup with an additional \mathbb{Z}_2 symmetry under which

$$\begin{aligned} X_{SM} &\rightarrow X_{SM}, & Q &\rightarrow Q, \\ (U, D) &\rightarrow -(U, D), & H_A &\rightarrow (-1)^A H_A. \end{aligned} \quad (3)$$

Under these transformations one is left with basically two \mathbb{Z}_2 -conserving sectors: one chiral (SM sector) and another VL, each one with its own scalar doublet. Thus, in this sense the SM and VL sectors are ‘‘orthogonal’’ up to scalar mixing, which can always be taken such that both sectors are decoupled. Note that in the absence of the VL fermions the resulting model would be a type-I 2HDM (see e.g. ref. [56] for further details).

It is well known that chiral-VL quark mixing is subject to several (stringent) constraints: In the up sector, these mixings induce e.g. deviations in the Zqq couplings which are severely constrained. First and second generation mixing are constrained by atomic parity violation experiments [57] and measurements of $R_c = \Gamma(Z \rightarrow \bar{c}c)/\Gamma(Z \rightarrow \text{hadrons})$ at LEP [57, 58], and are by far more stringent than those found for the third generation [59]. In the down sector the most severe constraints are derived from measurements of $R_b = \Gamma(Z \rightarrow \bar{b}b)/\Gamma(Z \rightarrow \text{hadrons})$, and so are stronger for third generation [59]. First and second down-type quark mixing are however severely constrained by meson mixing and decays [60]. In our setup, only color triplets enable writing \mathbb{Z}_2 -invariant renormalizable chiral-VL mixing terms. Indeed, an appealing feature of QCD exotics ($d_R = \mathbf{6}, \mathbf{8}, \mathbf{10}, \mathbf{15}$) is the intrinsic absence of renormalizable-induced chiral-VL mixing, assured by color invariance. Thus, in the triplet case, and only in that case, one has to worry about the size of the couplings controlling chiral-VL mixing. Two simple ways can be envisaged, either their values are phenomenologically fixed (can be fixed to zero) or the \mathbb{Z}_2 symmetry is promoted to a \mathbb{Z}_4 symmetry under which the SM fields and H_2 are neutral, while $Q \rightarrow -iQ$, $(U, D) \rightarrow i(U, D)$ and $H_1 \rightarrow -H_1$.² In what follows whenever referring to the color triplet we will assume the former.

Under the above working assumptions, the SM quarks combined with the H_2 doublet induce the following \mathbb{Z}_2 -invariant Yukawa interactions

$$\begin{aligned} -\mathcal{L}_Y^{\text{SM}} &= \bar{q}_L \cdot \mathbf{h}_u \cdot u_R \tilde{H}_2 + \bar{q}_L \cdot \mathbf{h}_d \cdot d_R H_2 \\ &+ \bar{\ell}_L \cdot \mathbf{h}_e \cdot e_R H_2 + \text{h.c.}, \end{aligned} \quad (4)$$

² For chiral quarks in the color triplet representation, a setup resembling in some aspects this one has been considered in ref. [61]

where $\mathbf{h}_{u,d,e}$ are the usual 3×3 Yukawa matrices in flavor space (we will denote matrices in boldface). In turn, the VL fermions combined with H_1 induce

$$-\mathcal{L}_Y^{\text{VL}} = \bar{Q}_L \cdot \mathbf{y}_U \cdot U_R \tilde{H}_1 + \bar{Q}_R \cdot \tilde{\mathbf{y}}_U \cdot U_L \tilde{H}_1 + \bar{Q}_L \cdot \mathbf{y}_D \cdot D_R H_1 + \bar{Q}_R \cdot \tilde{\mathbf{y}}_D \cdot D_L H_1 + \text{h.c.}, \quad (5)$$

where $\mathbf{y}_{U,D}$ and $\tilde{\mathbf{y}}_{U,D}$ are $n_{\text{VL}} \times n_{\text{VL}}$ matrices in the VL flavor space. Explicit mass terms are given in turn by:

$$-\mathcal{L}_m = \bar{Q}_L \cdot \hat{\mathbf{m}}_Q \cdot Q_R + \bar{U}_L \cdot \hat{\mathbf{m}}_U \cdot U_R + \bar{D}_L \cdot \hat{\mathbf{m}}_D \cdot D_R + \text{h.c.}, \quad (6)$$

where $\hat{\mathbf{m}}_Q$, $\hat{\mathbf{m}}_U$ and $\hat{\mathbf{m}}_D$ are $n_{\text{VL}} \times n_{\text{VL}}$ matrices in the VL flavor space which can be chosen to be diagonal without loss of generality.

Leading order (LO) VL fermion effects are controlled by the \mathbb{Z}_2 -invariant renormalizable interactions in (4)-(6). Higher order explicit \mathbb{Z}_2 -breaking effects are determined by non-renormalizable operators. For $d_R = \mathbf{3}, \mathbf{6}, \mathbf{15}$ those effects are determined by the dimension-six operators [62]³:

$$\mathcal{O}_6^{(1)} = \frac{C_6^{(1)}}{\Lambda^2} X_{d_R} q q \bar{q}, \quad \mathcal{O}_6^{(2)} = \frac{C_6^{(2)}}{\Lambda^2} X_{d_R} q \bar{q} \bar{q}, \quad (7)$$

where X_{d_R} stands for the VL colored fermion in the d_R representation and q refers to SM quark $SU(2)_L$ doublets or singlets, depending on the electroweak charges of X_{d_R} . For $d_R = \mathbf{8}, \mathbf{10}$, instead, effective LO effects are given by [62]:

$$\mathcal{O}_6^{(1)'} = \frac{C_6^{(1)'}}{\Lambda^2} X_{d_R} q q q, \quad \mathcal{O}_6^{(2)'} = \frac{C_6^{(2)'}}{\Lambda^2} X_{d_R} \bar{q} \bar{q} \bar{q}. \quad (8)$$

These operators are essential as they induce VL fermion decays, and so are responsible for the signatures one could expect at the LHC (see sec. III). Note however that when writing the effective operators in (7) and (8) one is implicitly assuming that the UV completion can indeed lead to such effective interactions, so to a large extent such effective approach is at any rate model-dependent. If the LO effective effects are instead determined by a different set of higher order effective operators (beyond six), the resulting picture will of course be different.

A further constraint of the new states that one has to bear in mind has to do with their contributions to electroweak precision data. Such contributions have been studied in ref. [63], where it has been shown—for the triplet case—that consistency with data it is always achievable. In the case of higher-order color representations one does not expect these conclusions to change since these contributions are color-blind.

At the scalar level, the presence of the \mathbb{Z}_2 symmetry constrains the scalar potential to have the form:

$$\mathcal{V} = m_{11}^2 H_1^\dagger H_1 + m_{22}^2 H_2^\dagger H_2 + \frac{\lambda_1}{2} (H_1^\dagger H_1)^2 + \frac{\lambda_2}{2} (H_2^\dagger H_2)^2 + \lambda_3 (H_1^\dagger H_1) (H_2^\dagger H_2) + \lambda_4 (H_1^\dagger H_2) (H_2^\dagger H_1) + \left[\frac{\lambda_5}{2} (H_1^\dagger H_2)^2 + \text{h.c.} \right]. \quad (9)$$

A. The CP-even Higgs mass matrix

We start by parametrizing the Higgs doublets according to:

$$H_{1,2} = \begin{pmatrix} H_{1,2}^+ \\ H_{1,2}^0 \end{pmatrix}, \quad (10)$$

where the neutral components are given by:

$$H_{1,2}^0 = \frac{1}{\sqrt{2}} (\varphi_{1,2}^0 + i\sigma_{1,2}^0 + v_{1,2}), \quad (11)$$

with $\langle H_{1,2}^0 \rangle = v_{1,2}/\sqrt{2}$, and $v^2 = v_1^2 + v_2^2 \simeq 246$ GeV. From the interactions in eq. (9), the CP even mass matrix in the basis $(\varphi_1^0, \varphi_2^0)$ can be written as:

$$\mathcal{M}_H^2 = \begin{pmatrix} m_{H_{11}}^2 & m_{H_{12}}^2 \\ m_{H_{12}}^2 & m_{H_{22}}^2 \end{pmatrix}, \quad (12)$$

with the different entries, assuming λ_5 to be real, given by

$$\begin{aligned} m_{H_{11}}^2 &= m_{11}^2 + \frac{1}{2} [3\lambda_1 v_1^2 + v_2^2 (\lambda_3 + \lambda_4 + \lambda_5)], \\ m_{H_{12}}^2 &= v_1 v_2 (\lambda_3 + \lambda_4 + \lambda_5), \\ m_{H_{22}}^2 &= m_{22}^2 + \frac{1}{2} [3\lambda_2 v_2^2 + v_1^2 (\lambda_3 + \lambda_4 + \lambda_5)]. \end{aligned} \quad (13)$$

Defining the mass eigenstate basis according to⁴

$$\begin{pmatrix} h \\ H \end{pmatrix} = \begin{pmatrix} -s_\alpha & c_\alpha \\ c_\alpha & s_\alpha \end{pmatrix} \begin{pmatrix} \varphi_1 \\ \varphi_2 \end{pmatrix} \equiv \mathbf{R}_S \begin{pmatrix} \varphi_1 \\ \varphi_2 \end{pmatrix}, \quad (14)$$

where $s_\alpha \equiv \sin \alpha$ and $c_\alpha \equiv \cos \alpha$, the diagonalization of the matrix in eq. (12) proceeds as follows

$$\mathbf{R}_S \cdot \mathcal{M}_H^2 \cdot \mathbf{R}_S^\dagger = \hat{\mathcal{M}}_H^2, \quad (15)$$

where the hat refers here and henceforth to diagonal matrices. The mixing angle reads

$$\tan 2\alpha = \frac{-2m_{H_{12}}^2}{m_{H_{22}}^2 - m_{H_{11}}^2}, \quad (16)$$

³ Higher order effective operators involving gluons are possible writing, see ref. [62] for further details.

⁴ In this notation h corresponds to the lightest CP even state.

while the mass eigenvalues are given by (assuming for definiteness $m_{H_{11}}^2 > m_{H_{22}}^2$):

$$m_{h(H)}^2 = \frac{1}{2} \left(\Delta m_{\pm}^2 \mp \sqrt{\Delta m_{\pm}^4 + 4m_{H_{12}}^4} \right), \quad (17)$$

with Δm_{\pm}^2 defined according to

$$\Delta m_{\pm}^2 = m_{H_{11}}^2 \pm m_{H_{22}}^2. \quad (18)$$

Notice that in the limit $m_{H_{11}}^2 \gg m_{H_{22}}^2 > m_{H_{12}}^2$ we get:

$$m_h^2 \simeq m_{H_{22}}^2 - \frac{m_{H_{12}}^2}{m_{H_{11}}^2}, \quad (19)$$

$$m_H^2 \simeq m_{H_{11}}^2, \quad (20)$$

and small mixing angle α , see eq. (16), so that $h \sim \varphi_2$, and $H \sim \varphi_1$. Finally, the CP-odd Higgs mass can be written as

$$m_{A_0}^2 = m_H^2 + \lambda_5 v_2^2. \quad (21)$$

We stress that in the following we will fix $m_h = 125$ GeV and $1.8 < m_H < 2.2$ TeV.

As usual, the CP odd Higgses mass matrix is diagonalized by a 2×2 unitary matrix parametrized with $\tan \beta = v_2/v_1$. Of relevance for the process we will consider in Sec. III are the couplings for WWh , WWH , ZZh and ZZH [55]:

$$g_{VVh} = \frac{2M_V^2}{v} s_{\alpha-\beta}, \quad g_{VVH} = \frac{2M_V^2}{v} c_{\alpha-\beta}. \quad (22)$$

B. VL quark mass matrices

In the presence of n_{VL} VL fermion generations, the $2n_{\text{VL}} \times 2n_{\text{VL}}$ mass matrix, written in the left-right bases, with these bases defined as $(\psi_{L,R}^U)^T = (\tilde{U}_{L,R}, U_{L,R})$, reads:

$$\mathcal{M}_U = \begin{pmatrix} \hat{m}_Q & \bar{m}_U \\ \tilde{\bar{m}}_U^\dagger & \hat{m}_U \end{pmatrix}, \quad (23)$$

where the following notation has been used:

$$\bar{m}_U = \frac{v}{\sqrt{2}} c_\beta \mathbf{y}_U, \quad \tilde{\bar{m}}_U = \frac{v}{\sqrt{2}} c_\beta \tilde{\mathbf{y}}_U, \quad (24)$$

The down-type sector mass matrix, in the bases $(\psi_{L,R}^D)^T = (\tilde{D}_{L,R}, D_{L,R})$, follows the same structure, namely

$$\mathcal{M}_D = \begin{pmatrix} \hat{m}_Q & \bar{m}_D \\ \tilde{\bar{m}}_D^\dagger & \hat{m}_D \end{pmatrix}. \quad (25)$$

The parameters \bar{m}_D and $\tilde{\bar{m}}_D$ are given by those in (24) by trading the subindex $U \rightarrow D$.

Defining the mass eigenstate bases as

$$\Psi_L^{(U,D)} = \mathbf{R}_L^{(U,D)} \psi_L^{(U,D)}, \quad \Psi_R^{(U,D)} = \mathbf{R}_R^{(U,D)} \psi_R^{(U,D)}, \quad (26)$$

both matrices can therefore be diagonalized through bi-unitary transformations:

$$\mathbf{R}_L^{(U,D)} \cdot \mathcal{M}^{(U,L)} \cdot \mathbf{R}_R^{(U,D)\dagger} = \hat{\mathcal{M}}^{(U,L)}. \quad (27)$$

C. Relevant Higgs couplings

Recasting the interactions in eq. (5) in the mass eigenstates bases for both, the VL fermions and H_1 , one gets for the LR couplings

$$\begin{aligned} \mathcal{L}_{LR} = & \sum_{a,b=1}^{2n_{\text{VL}}} \bar{\Psi}_{L_a}^U O_{ab}^{ULR} \kappa_A \Psi_{R_b}^U S_A \\ & + \sum_{a,b=1}^{2n_{\text{VL}}} \bar{\Psi}_{L_a}^D O_{ab}^{DLR} \kappa_A \Psi_{R_b}^D S_A + \text{h.c.}, \end{aligned} \quad (28)$$

where for $A = 1$, $\kappa_1 = -s_\alpha$ and $S_1 = h$, while for $A = 2$, $\kappa_2 = c_\alpha$ and $S_2 = H$. The couplings for the up- and down-type sectors are given by

$$\begin{aligned} O_{ab}^{ULR} &= R_{L_{ac}}^U Y_{U_{cd}} R_{R_{bd}}^{U*}, \\ O_{ab}^{DLR} &= R_{L_{ac}}^D Y_{D_{cd}} R_{R_{bd}}^{D*}. \end{aligned} \quad (29)$$

Here $\mathbf{Y}_{X_{cd}}$ are the elements of the $2n_{\text{VL}} \times 2n_{\text{VL}}$ matrix

$$\mathbf{Y}_X = \begin{pmatrix} \mathbf{0}_{n_{\text{VL}}} & \mathbf{y}_X \\ \tilde{\mathbf{y}}_X^\dagger & \mathbf{0}_{n_{\text{VL}}} \end{pmatrix}, \quad (30)$$

with $X = U, D$ and $\mathbf{0}_{n_{\text{VL}}}$ a $2n_{\text{VL}} \times 2n_{\text{VL}}$ matrix with vanishing elements. Summation over repeated indices is assumed in eq. (29).

A simple case of interest for our phenomenological analysis is that where $n_{\text{VL}} = 1$. In that case, the couplings y_X and \tilde{y}_X can be taken to be real without loss of generality. Thus, the matrices $\mathbf{R}_{L,R}^{(U,D)}$ can be parameterized according to

$$\mathbf{R}_{L,R}^{(X)} = \begin{pmatrix} \cos \theta_{L,R}^X & \sin \theta_{L,R}^X \\ -\sin \theta_{L,R}^X & \cos \theta_{L,R}^X \end{pmatrix} \quad (X = U, D), \quad (31)$$

with the corresponding mixing angles given by

$$\begin{aligned} \tan 2\theta_L^X &= -2 \frac{m_Q \tilde{m}_X + m_X \bar{m}_X}{m_X^2 - m_Q^2 - \tilde{m}_X^2 + \bar{m}_X^2}, \\ \tan 2\theta_R^X &= -2 \frac{m_Q \bar{m}_X + m_X \tilde{m}_X}{m_X^2 - m_Q^2 - \tilde{m}_X^2 + \bar{m}_X^2}. \end{aligned} \quad (32)$$

With the aid of eq. (31), the interactions in eq. (28) written in the mass eigenstate basis are given by

$$\begin{aligned} \mathcal{L}_U = & \frac{\kappa_A}{\sqrt{2}} \left(Y_{11}^U \bar{U}'_L \tilde{U}'_R + Y_{12}^U \bar{U}'_L U'_R \right. \\ & \left. + Y_{21}^U \bar{U}'_L U'_R + Y_{22}^U \bar{U}'_L U'_R \right) S_A + \text{h.c.}, \end{aligned} \quad (33)$$

where the different couplings read:

$$Y_{11}^U = y_U \cos \theta_L^U \sin \theta_R^U + \tilde{y}_U \cos \theta_R^U \sin \theta_L^U, \quad (34)$$

$$Y_{12}^U = y_U \cos \theta_L^U \cos \theta_R^U - \tilde{y}_U \sin \theta_L^U \sin \theta_R^U, \quad (35)$$

$$Y_{21}^U = -y_U \sin \theta_L^U \sin \theta_R^U + \tilde{y}_U \cos \theta_L^U \cos \theta_R^U, \quad (36)$$

Standard Model		
Couplings	u sector ($f = u$)	d sector ($f = d$)
$g_{f_i f_i h}$	$(m_{u_i}/v)(c_\alpha/s_\beta)$	$(m_{d_i}/v)(c_\alpha/s_\beta)$
$g_{f_i f_i H}$	$(m_{u_i}/v)(s_\alpha/s_\beta)$	$(m_{d_i}/v)(s_\alpha/s_\beta)$
Vector-like		
Couplings	U sector ($F = U$)	D sector ($F = D$)
$g_{F_i F_j h}$	$Y_{ij}^U s_\alpha$	$Y_{ij}^D s_\alpha$
$g_{F_i F_j H}$	$Y_{ij}^U c_\alpha$	$Y_{ij}^D c_\alpha$

TABLE I. Yukawa couplings for SM and VL up- and down-type quarks. Note that enhanced $g_{F_i F_j H}$ couplings ($c_\alpha \rightarrow 1$) guarantee negligible $g_{F_i F_j h}$ parameters.

$$Y_{22}^U = - (y_U \sin \theta_L^U \cos \theta_R^U + \tilde{y}_U \cos \theta_L^U \sin \theta_R^U). \quad (37)$$

Those in the down-type sector have the form

$$\begin{aligned} \mathcal{L}_D = \frac{\kappa_A}{\sqrt{2}} & \left(Y_{11}^D \overline{\widetilde{D}}'_L \widetilde{D}'_R + Y_{12}^D \overline{\widetilde{D}}'_L \widetilde{D}'_R \right. \\ & \left. + Y_{21}^D \overline{\widetilde{D}}'_L D'_R + Y_{22}^D \overline{\widetilde{D}}'_L D'_R \right) S_A + \text{h.c.}, \quad (38) \end{aligned}$$

with the down-type sector couplings given as in (34)-(37) trading $U \rightarrow D$. The primes refer to the fields written in the mass basis.

As we have already pointed out, the symmetry transformations in eq. (3) allow the chiral (SM) and VL sectors to be decoupled in such a way that VL couplings can not sizeably affect the SM Higgs single production cross-section. This can be seen in tab. I, where we have listed the couplings of both sectors according to the interactions in (33) and (38). In the limit $\sin \alpha \rightarrow 0$ any such contribution will vanish, while those related with the heavy CP-even scalar H will be enhanced. This is, in our opinion, an interesting feature of our setup: the condition of large contributions to the H single production cross-section assures negligible (or even vanishing) contributions to the SM h single production.

III. PHENOMENOLOGICAL ANALYSIS

Higgs properties derived from production and decay mode analyses at LHC have placed stringent bounds on 2HDMs [64–66]. Although consistency with data still allows for certain freedom, favored regions in parameter space are those corresponding to the decoupling limit [64], in which apart from h (whose mass is fixed to ~ 125 GeV [67, 68]) the remaining part of the scalar mass spectrum is heavy [55]. In terms of the scalar sector mixing angles, this translates into small $\cos(\alpha - \beta)$, with the possible values for $\tan \beta$ depending on the model itself [66, 69]. For the type-I 2HDM, which corresponds in our case to the SM sector, values of $\sin(\alpha - \beta)$ close to 1 do not necessarily demand large values of $\tan \beta$, as it turns out to be e.g. in the type-II 2HDM [69].

The heavier CP-even state H can be produced solely through SM interactions, as can be noted from tab. I. However, the corresponding cross-section in that case is expected in general to be small, as can be seen by going to the decoupling limit. Since in that case $\alpha = \beta + \pi/2$, g_{ttH} matches the SM coupling. The coupling g_{ttH} , instead, becomes $(m_t/v) \cot \beta$, which even for moderate values of $\tan \beta$ implies a suppressed production cross-section. Thus, sizeable production of H is only possible through the VL couplings. As can be seen in tab. I, both g_{FFh} and g_{FFH} in that case are not sensitive to values of $\tan \beta$, suppressed (enhanced) production of h (H) can be achieved solely through small (large) values of s_α (c_α). Thus, one can consistently get enhanced H production without considerably affecting h production.

The gluon fusion H production cross-section strongly depends on the VL fermion mass spectrum. The dependence enters in two ways, namely. The loop function combined with the fact that in this case the Yukawa couplings are not directly related with the VL fermion masses, induce a decoupling behavior which for heavy VL mass spectra strongly suppresses the cross-section. Secondly, depending on the VL and scalar mass spectra, the new states can sizeably contribute to the running of α_s , largely changing its value (for more details see sec. III A).

In summary, as what regards H production, consistency with data requires being close to the decoupling limit. This condition implies suppressed g_{ffH} couplings which then demands H production through VL couplings. The contributions of these couplings to the gluon fusion h production cross-section are small (or can even vanish), so it is possible to achieve a consistent picture of “large” H production.

CP-odd scalar production proceeds in the same way, controlled by the same set of parameters. The only difference resides in the mass difference between the heavy CP-even and the CP-odd scalar, which due to the constraints implied by the scalar potential are small: taking the non-perturbative limit value $\lambda_5 = 4\pi$, one gets the bound (see eq. (21)):

$$m_A \lesssim 2.3 \text{ TeV}, \quad (39)$$

a value in agreement with electroweak precision data.

A. Production cross-section and VL fermion mass limits

In the case $n_{VL} = 1$ there are two different contributions to $\sigma(pp \rightarrow H)$ for both, the up- and down-type VL sectors. The contributions are determined by the first and fourth terms in eqs. (33) and (38). The gluon fusion cross-section then has the form

$$\hat{\sigma}(gg \rightarrow H) = \frac{\kappa \alpha_s^2}{64 \pi} \cos^2 \alpha \left| T_R \sum_{\substack{X=U,D \\ i=1,2}} \frac{Y_{ii}^X}{\sqrt{2}} \frac{A(m_H^2/m_{X_i}^2)}{m_{X_i}} \right|^2$$

Cross-section

$$\times \tau_0 \delta(\tau - \tau_0) . \quad (40)$$

Here we have included a κ factor to account for NLO corrections and defined $\tau = s/S$ and $\tau_0 = m_H^2/S$, where s and S are the parton-parton and proton-proton center of mass energies, respectively. In our numerical analysis we will fix $\sqrt{S} = 8$ TeV. The ‘‘effective’’ couplings $Y_{ii}^{U,D}$ are given by eqs. (34) and (37) and encode the dependence of the cross-section upon the VL Yukawa couplings and VL fermion mixing. The loop function $A(m_H^2/m_{X_i}^2)$ reads

$$A(m_H^2/m_{X_i}^2) = \int_0^1 dy \int_0^{1-y} dz \frac{1 - 4yz}{1 - (m_H^2/m_{X_i}^2)yz} , \quad (41)$$

and match after integration the standard one-loop functions for Higgs production via gluon fusion (see e.g. ref. [70]).

The physical cross-section at the LHC requires integration over the parton distribution functions $g(x)$:

$$\sigma(pp \rightarrow H) = \int_{\tau_0}^1 dx_1 \int_{\tau_0/x_1}^1 dx_2 g(x_1) g(x_2) \hat{\sigma}(gg \rightarrow H) . \quad (42)$$

Some words are in order regarding the group theory factors T_R . The gluon-VL-VL coupling structure is determined by the $SU(3)_c$ generators t_R^a , which in turn depend upon the VL irreducible representation R , assumed to be of rank (λ_1, λ_2) . The amplitude for the gluon fusion process, therefore, involves $\text{Tr}(t_R^a t_R^b)$, whose value is given by the trace normalization condition:

$$\text{Tr}(t_R^a t_R^b) = \frac{C_R d_R}{d_A} \delta^{ab} = T_R \delta^{ab} , \quad (43)$$

where d_R and d_A refer to the dimensions of the representation R and the adjoint ($A = \mathbf{8}$), and C_R is the constant that defines the quadratic Casimir, namely

$$\begin{aligned} d_R &= \frac{1}{2}(\lambda_1 + 1)(\lambda_2 + 1)(\lambda_1 + \lambda_2 + 2) , \\ C_R &= \frac{1}{3}(\lambda_1^2 + \lambda_2^2 + \lambda_1 \lambda_2 + 3\lambda_1 + 3\lambda_2) . \end{aligned} \quad (44)$$

Bearing in mind that the adjoint is rank (1,1), T_R is entirely determined by the rank of the corresponding representation, namely: $\mathbf{3} = (1, 0)$, $\mathbf{6} = (2, 0)$, $\mathbf{10} = (3, 0)$ and $\mathbf{15} = (2, 1)$. Values for d_R , C_R and T_R for the lower-dimensional $SU(3)$ representations are given in tab. II.

We discuss now the evolution of α_s under the Renormalization Group Equations (RGEs). In the absence of the new colored states (SM alone) we find $\alpha_s(M_Z)/\alpha_s(m_H) = \{1.40, 1.42, 1.43\}$ for $m_H = \{1.8, 2.0, 2.2\}$ TeV (the values used in our numerical treatment). The VL fermions, in particular those belonging to higher order color representations, can substantially change those values through their non-negligible positive contributions to the RGE running. Whether this is the case depends on the corresponding VL mass spectrum. For spectra heavier than m_H there is no contribution, thus the values previously quoted are the ones to be

used. For spectra with at least one VL state with mass below m_H , the α_s RGE running should be accounted for, as it may have a non-negligible numerical impact on the resulting H production cross-section. The α_s RGE reads:

$$\mu \frac{d\alpha_s}{d\mu} = \alpha_s \sum_i \beta_i \left(\frac{\alpha_s}{\pi} \right)^i , \quad (45)$$

with the one- and two-loop β functions given by [71, 72]

$$\beta_1 = -\frac{11}{6} C_A + \frac{2}{3} \sum_R n_R T_R , \quad (46)$$

$$\beta_2 = -\frac{17}{12} C_A^2 + \frac{1}{6} \sum_R n_R T_R (5 C_A + 3 C_R) , \quad (47)$$

where n_R is the number of quark flavors in the representation R . Clearly, the higher the rank of the representation (large T_R and C_R), the larger the contribution of the VL states to α_s . Indeed, it can be noted that for higher rank representations a Landau pole will be reached rapidly, implying in those cases the need for further color states with order-TeV masses, so to assure a good UV behavior.

Having accounted for all the relevant effects, it becomes clear that the gluon fusion Higgs production cross-section for different representations differ solely by the group theory factor and the value of α_s at m_H . Thus, as soon as its value is determined for a particular representation, values for the others can be straightforwardly derived by rescaling by the appropriate factors. Relative to the fundamental representation, $F = \mathbf{3}$, these factors are

$$\varepsilon_{gg}^H \equiv \frac{\sigma_R(gg \rightarrow H)}{\sigma_F(gg \rightarrow H)} = \frac{T_R^2}{T_F^2} \frac{\alpha_{s,R}^2}{\alpha_{s,F}^2} . \quad (48)$$

Tab. II shows the group theory enhancements for the irreducible representations of interest, from which it can be seen that large cross-sections are expected for higher-rank representations. This is however subtle, since large cross-sections demand not too heavy VL states. And is for higher rank representations for which one could expect the most stringent bounds on their masses. This statement is, however, to a large extent, model-dependent. Bounds are derived assuming certain VL fermion decay modes, which in the absence of chiral-VL mixing entirely depend upon the effective operator assumed, as we now discuss.

VL fermions pair-production is mainly driven by $gg \rightarrow X\bar{X}$. At leading order in m_X^2/S , the production cross-sections for representations R_a and R_b differ by [54]:

$$\varepsilon_{gg}^{(R_a, R_b)} \equiv \frac{\sigma(gg \rightarrow X_a \bar{X}_a)}{\sigma(gg \rightarrow X_b \bar{X}_b)} \simeq \frac{C_{R_a}^2}{C_{R_b}^2} \frac{d_{R_a}}{d_{R_b}} . \quad (49)$$

Such values are shown in tab. II relative to the fundamental representation. With the aid of these rescaling factors, bounds on the masses of different representations can be indirectly estimated from experimental bounds

$SU(3)_c$ representations					
d_R	3	6	8	10	15
C_R	4/3	10/3	3	6	16/3
T_R	1/2	5/2	3	15/2	10
$\varepsilon_{gg}^H \times \alpha_{S,F}^2 / \alpha_{S,R}^2$	1	25	36	225	400
$\varepsilon_{gg}^{(R,F)}$	1	25/2	27/2	135/2	80

TABLE II. Dimension d_R , quadratic Casimir operators coefficient (C_R) and trace factor (T_R) for lower-dimensional color representations. The coefficient ε_{gg}^H refers to the enhancement of the heavy Higgs gluon fusion cross-section for representations $R = 6, 8, 10, 15$, relative to the fundamental representation ($F = 3$). The other coefficient $\varepsilon_{gg}^{(F,X)}$ refers instead to the enhancement of the VL pair production cross-section $\sigma(gg \rightarrow X\bar{X})$. Note that, in the Higgs gluon fusion enhancement coefficient, α_s has been evaluated at m_H . See text for further details.

on the mass of a given one. Such an approach assumes the VL fermions to be short-lived, with lifetimes below 10 ns. For lifetimes above this value (and below ~ 100 s, as required by cosmological and astrophysical constraints [73]), the VL fermions would be stable or metastable depending on whether they decay outside or inside the active detector volume [74]. In that case, arguably, bounds on the different VL fermions could be fixed by using current bounds on charged heavy long-lived particles, for which current bounds exclude masses below ~ 1 TeV [74].

VL fermion lifetimes are determined by the effective operator responsible for its decay (see sec. II). Assuming $\mathcal{O}(C_6, C'_6) \sim 1$ and taking $m_X = 1.5$ TeV, we have found that short-lived VL fermions are obtained for cutoff scales obeying $\Lambda \lesssim 10^7$ GeV, stability at collider scales is instead obtained for 10^7 GeV $\lesssim \Lambda \lesssim 10^{10}$ GeV (where the upper bound assures decay lifetimes below 100 s).

In the short-lived case, mass limits for the different representations can be derived by using current bounds on gluino masses in models with R-parity violation [75]. These limits, derived from searches for six jets stemming from R-parity-violating gluino decays, have excluded gluino masses below ~ 900 GeV. Since the gluino is a VL octet, these bounds combined with appropriate rescaling factors can—in principle—be used to derive lower limits on the remaining VL quark representations, provided the VL decay modes yield a six jet topology. This is indeed the case for decays induced by the effective operators in (7) and (8). Thus, in that case for

$$\begin{aligned} \varepsilon_{gg}^{(F,A)} &= \frac{2}{25}, & \varepsilon_{gg}^{(6,A)} &= \frac{25}{27}, \\ \varepsilon_{gg}^{(10,A)} &= \frac{27}{5}, & \varepsilon_{gg}^{(15,A)} &= \frac{32}{5}, \end{aligned} \quad (50)$$

we find no competitive bound for m_{X_3} (so its lower value is then fixed to 500 GeV [76]), for $m_{X_6} \gtrsim 833$ GeV and for $m_{X_{10}, X_{15}} \gtrsim 4000$ GeV. The latter, being at the LHC kinematical threshold, is therefore expected to be some-

what degraded.

The octet having a weaker mass bound and an expected large cross-section, it is probably the most suitable VL fermion for addressing the ATLAS diboson excess (in the case of short-lived VL fermions). Thus, most of our results in sec. III C will specialize to this case.

Finally, before closing this section it is worth pointing out that the above limits imply a depletion of the gluon fusion cross-section for the different representations, apart from the triplet for which less stringent bounds apply. This is to be compared with the case where the states rather than being VL are chiral, since constraints on a fourth chiral quark generation are less restrictive, $m_{\text{chiral}} \gtrsim 600$ GeV [77]⁵, and the cross-section does not exhibit a decoupling behavior. Note, however, that in that case addressing the diboson anomaly is not possible: the large Yukawa couplings required to generate experimentally consistent chiral masses necessarily lead to a heavy Higgs total decay width above ~ 200 GeV (see next section).

B. Partial decay widths

The dominant H decay modes are: $H \rightarrow VV$ ($V = W, Z$), $H \rightarrow X_i \bar{X}_j$ (see ecs. (33) and (38)). The partial decay widths for these processes can be written as:

$$\Gamma(H \rightarrow VV) = \frac{\delta_V G_F}{16\sqrt{2}\pi} m_H^3 c_{\alpha-\beta}^2 G(1, r_{VH}^2, r_{VH}^4), \quad (51)$$

$$\Gamma(H \rightarrow X_i \bar{X}_i) = \frac{d_R}{8\pi} \frac{|Y_{ii}^X|^2}{2} m_H \lambda^{3/2}(1, r_{X_i H}^2, r_{X_i H}^2), \quad (52)$$

$$\Gamma(H \rightarrow X_i \bar{X}_j) = \frac{d_R}{8\pi} \frac{|Y_{ij}^X|^2}{2} m_H F(1, r_{X_1 H}^2, r_{X_2 H}^2). \quad (53)$$

Here $\delta_V = 2$ for $V = W$ and $\delta_V = 1$ for $V = Z$, $i = 1, 2$ refer to the states in the up and down sector, Y_{ij}^X are the off-diagonal couplings given in (35) and (36), $r_{VH} = m_V/m_H$, $r_{X_i H} = m_{X_i}/m_H$ and the kinematic functions read

$$\begin{aligned} G &= (1 - 4r_{VH}^2 + 12r_{VH}^4) \lambda^{1/2}(1, r_{VH}^2, r_{VH}^2), \\ F &= [1 - (r_{X_1 H} + r_{X_2 H})^2] \lambda^{1/2}(1, r_{X_1 H}^2, r_{X_2 H}^2), \end{aligned} \quad (54)$$

with $\lambda(1, a, b) = 1 + (a - b)^2 - 2(a + b)$.

Depending on the relative size of $\cos(\alpha - \beta)$ and the “effective” couplings $Y_{ij}^{U,D}$ ($i = 1, 2$), the total decay width

⁵ Within our setup, a fourth chiral generation coupling only to H_1 is absolutely viable, since its contribution to the SM Higgs cross-section is negligible or even vanishing.

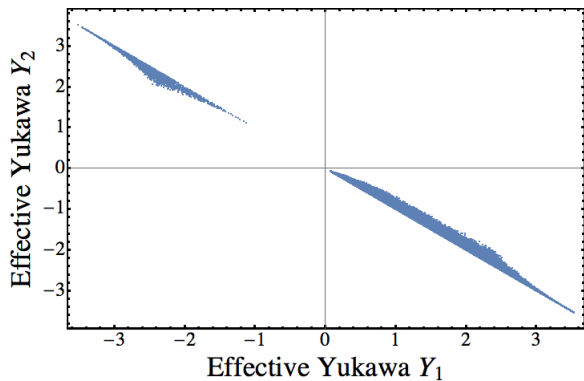


FIG. 1. Regions of heavy Higgs cross-section as a function of the effective couplings Y_1 and Y_2 for octet VL fermions. The cross-section distribution over the plane is such that the larger the “effective” couplings the larger the cross-section.

is controlled either by gauge boson modes or fermion decays. For higher representations, fermion decay dominance is more pronounced due to the largest number of color degrees of freedom. However, in general, for “effective” couplings $Y_{ij}^{U,D}$ smaller than one the gauge boson modes dominate, unless $\cos(\alpha - \beta) \lesssim 0.01$. On the contrary, for large “effective” couplings, fermion modes can determine the total decay width, with the corresponding value typically being well above ~ 100 GeV.

C. Numerical results

No matter the color representation, the heavy Higgs gluon fusion cross-section depends on the VL mixing as well as on the VL fermion mass spectrum (in both up- and down-type sectors). Their values are to a large extent correlated since they both depend upon the same set of Lagrangian parameters, and although they depend differently there is no room for variations on the mixing giving a mass spectrum. Thus, rather than treating mixing and spectrum independently, in our analysis we used the “fundamental” couplings, assuming common values for both sectors. Such an assumption certainly simplifies the numerical treatment, while capturing the main features of the parameter space dependence. Our results are therefore derived for fixed $m_H = 1.8$ TeV and $\sqrt{S} = 8$ TeV and are based on random scans of the following parameter space regions:

$$\begin{aligned} m_{Q,X} &\in [500, 2500] \text{ GeV}, & y, \tilde{y} &\in [10^{-1}, \sqrt{4\pi}], \\ \tan\beta &\in [0.3, 10], & \sin(\alpha - \beta) &\in [0.9, 1]. \end{aligned} \quad (55)$$

For all points in the scan we have calculated (for each representation) the exact value for α_s making use of eqs. (45) and (46). In doing so, we have accounted for the decoupling of the different VL fermions at their mass

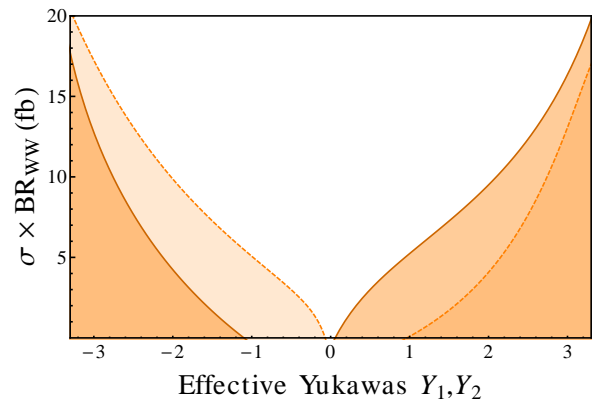


FIG. 2. Signal $\sigma(pp \rightarrow H) \times \text{Br}(H \rightarrow W^+W^-)$ as a function of the effective couplings Y_1 (dashed orange) and Y_2 (solid brown) for octet VL fermions.

thresholds. For higher representations, in particular for **10** and **15**, a VL fermion mass way below m_H can lead to non-perturbative α_s already at m_H . Whenever those points are found we just drop them from our analysis. If not stated otherwise, all our points are subject to the cut $\Gamma_H < 200$ GeV, where Γ_H is the heavy Higgs total decay width. Finally, for the calculation of the cross-section we have used the MSTW PDFs at NNLO [78].

The different “effective” couplings entering in (40) are weighted by different signs, with the sign difference holding regardless of the region in parameter space, as shown in fig. 1. This effect leads to a certain degree of cancellation of the different terms in the cross-section, something that happens as well in the presence of color scalars as has been pointed out in [79]. As an illustration of this cancellation, one can look at the particular case of $y_U = \tilde{y}_U \equiv y$. In this case the mass matrix in eq. 23 is symmetric, and $\theta_R^U = \theta_L^U \equiv \theta$. Therefore, the effective Yukawas entering eq. (33) read $Y_{11}^U = -Y_{22}^U = y \sin(2\theta)/2$. One can then clearly see that a cancellation in both, the up- and down-type sectors contributions occurs up to mass non-degeneracy.

Several factors, however, “compensate” for such cancellation, and can be sorted depending on whether they are or not representation-dependent. Non representation-dependent correspond to size of Yukawa couplings and VL fermion mass spectrum⁶. Group theory factors and α_s running are, instead, representation-dependent, and are such that for representations beyond the triplet they lead to sizeable enhancements. It is worth pointing out that for the fundamental representation, and only for that representation, the “compensating” factors do not suffice to render this possibility viable. However, if not for this cancellation effect the fundamental color rep-

⁶ Note, however, that the constraints on the mass spectrum are representation-dependent, and so indirectly it features a representation dependence.

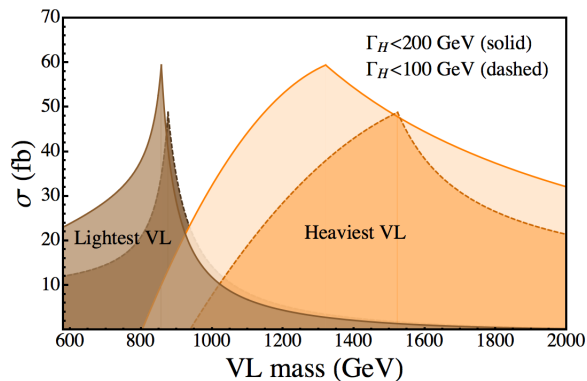


FIG. 3. Gluon fusion cross-section versus the two octet VL fermion masses: the brownish region is for the lightest and the orangish for the heaviest. The different shaded regions correspond to the “cuts” $\Gamma_H < 100$ GeV and $\Gamma_H < 200$ GeV and show the constraints on the cross-section due to the condition of “narrow” resonance.

resentation alone could account for the diboson excess anomaly.

The larger the Yukawa couplings (y and \tilde{y}) the larger the expected cross-section. We illustrate this in figure 2, where we plot $\sigma(pp \rightarrow H) \times \text{Br}(H \rightarrow W^+W^-)$ as a function of the effective couplings Y_1 (dashed orange) and Y_2 (solid brown), for octet VL fermions and $\Gamma_H \lesssim 200$ GeV. Note that the Yukawas are typically $\mathcal{O}(1)$ at m_H ⁷. Thus, their RGE running could lead in some cases to non-perturbative couplings or vacuum instabilities at scales not-too-far from m_H , as it turns out to be with α_S . In that case, new degrees of freedom would be needed to render our picture consistent at high energies.

However, large Yukawa couplings not only enhance the cross-section but can potentially render the heavy Higgs total decay width well above its maximum allowed value, $\Gamma_H \sim 200$ GeV. The “narrow” width condition places a strong constraint on the possible values of the Yukawa couplings, with the effect being more pronounced for higher representations. The reason is rather simple. While only two Yukawa vertices contribute to the gluon fusion cross-section (first and fourth terms in eqs. (33) and (38), for $A = 2$), four contribute to Γ_H , determined by partial decay widths weighted by final state multiplicities, whose values scale with the dimension of the representation. In fig. 3, we display results for the gluon fusion cross-section as a function of the two octet VL fermion masses: the brownish region is for the lightest and the orangish for the heaviest. The results correspond to two different “cuts”, determined by $\Gamma_H < 100$ GeV and $\Gamma_H < 200$ GeV. This shows that indeed the smaller Γ_H , the smaller the cross-section. Furthermore, the role of

⁷ One has to bear in mind that in models with higher $SU(3)_c$ representations κ is expected to be larger than 2, and with larger κ factors the Yukawa couplings will decrease accordingly.

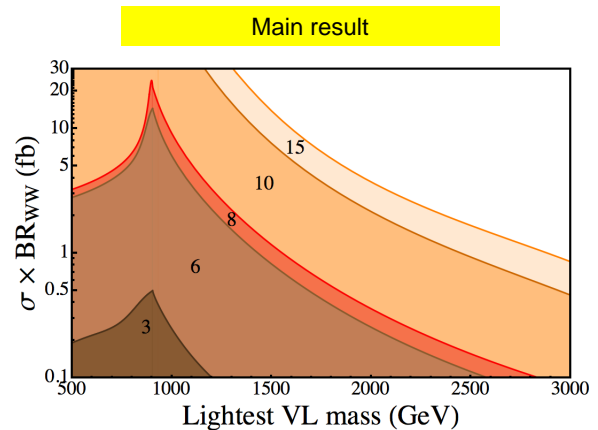


FIG. 4. Signal $\sigma(pp \rightarrow H) \times \text{Br}(H \rightarrow W^+W^-)$ as a function of the lightest VL fermion for the five color representations we have employed. The different shaded regions from bottom to top correspond to: **3, 6, 8, 10, 15**.

kinematically open/closed Higgs fermion channels is also striking. In those regions of “light” states ($m_{X_1} < m_H/2$) the cross-section is small and increases towards values approaching the fermion modes kinematical threshold, reaching a maximum determined by the loop function $A(m_H^2/m_X^2)$ and decreasing due to the expected decoupling behavior of the cross-section.

Representation-dependent effects are obvious but remarkable. As shown in tab. II, the heavy gluon fusion cross-section rapidly increases with higher representations. Thus, alone, the group theory factor could “overcome” the cancellation effect. **However, higher representations in turn are, in the case of prompt decays, subject to more stringent experimental constraints, thus being more sensitive to the cross-section decoupling behavior.** With the bounds we derived in sec. III A for short-lived VL fermions, we find that while the sextet and octet lead to a signal, $\sigma(pp \rightarrow H) \times \text{Br}(H \rightarrow W^+W^-)$, in agreement with the ATLAS reported excess, **10 and 15 do not.** Such statement is only valid when those mass bounds hold, deviations from those values will of course change the conclusion. For example, if these representations are long-lived their mass limits will not be so stringent, allowing them to perfectly fit the ATLAS anomaly (see the discussion in sec. III A). For that reason, we do not discard the possibility of **10 and 15** VL fermions *a priori* and calculate the signal for all the representations listed in tab. II.

Fig. 4 shows the results for the five representations we are considering. Their relative values agree very well with those expected from group theory, see table II. This result clearly shows that the fundamental representation cannot, by any means, account for the ATLAS excess. Even relying on the mass bounds derived for short-lived fermions, the sextet and octet can readily address the ATLAS observation provided $m_{X_{6,8}} \lesssim 1.5$ TeV. The **10** and **15** can account for the anomaly depending on their

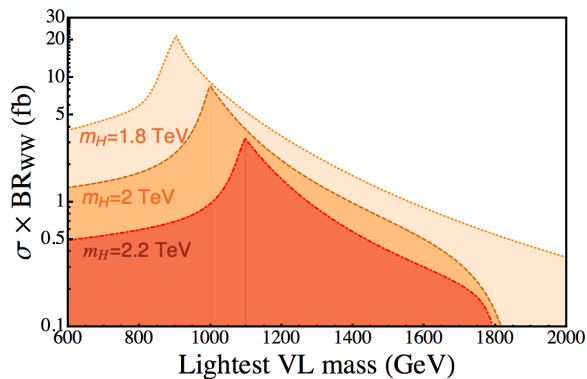


FIG. 5. Signal $\sigma(pp \rightarrow H) \times \text{Br}(H \rightarrow W^+W^-)$ as a function of the lightest VL fermion for the octet. The different shaded regions from top to bottom correspond to: $m_H = 1.8, 2$ and 2.2 TeV.

mass limits.⁸ For masses of up to about ~ 2.5 TeV, both representations can fit the observed ATLAS signal (with a somewhat marginal fit at 2.5 TeV). For masses above those values the decoupling effect is stringent and the signal is degraded below 1 fb, way below the values indicated by ATLAS. For those representations too, one may wonder about the extremely “large” signal at low VL fermion masses: such values can be fitted to those required to address the anomaly by properly decreasing the values of the Yukawa couplings.

The heavy Higgs gluon fusion cross-section dependence on m_H is as well somewhat strong. Thus, since the results presented so far are for $m_H = 1.8$ TeV, we have investigated up to which extent the octet and sextet can or not account for the signal in the relevant experimental range, [1.8, 2.2] TeV. Note that in the low mass region the **10** and **15** are expected to always be able to address the anomaly, regardless of the Higgs mass. Fig. 5 shows the results for the octet case for three different values of $m_H : 1.8, 2.0, 2.2$ TeV. Although the signal is depleted about an order of magnitude when moving from 1.8 TeV to 2.2 TeV, it is still possible to obtain a signal within the range reported by ATLAS.

IV. CONCLUSIONS

We have shown that the diboson excess reported by ATLAS (and CMS) might be due to the production and further decay of a heavy Higgs, H , resulting from a type-I 2HDM. Production proceeds through gluon fusion, enhanced by the presence of colored VL fermion. In addition to “standard” color triplets, we have considered as well higher-order color representations (QCD exotics) which we have taken to be **6**, **8**, **10** and **15**. Our findings show that barring the triplet case (in its minimal form), all other representations lead to large cross-sections in

fairly large portions of the parameter space.

We have studied constraints on VL fermion masses, which we have argued depend upon their lifetime. However, no matter whether the new states are short- or long-lived we have found that—in general—phenomenological consistency requires their masses to be above 1 TeV. These limits then translates into heavy Higgs decays dominated by gauge boson modes, thus naturally yielding the $W^\pm W^\mp$ and $Z^0 Z^0$ diboson signal observed by ATLAS.

The different scenarios we have considered can be regarded as minimal. Additional VL fermion generations could be considered as well, and in those cases enhancements of the cross-section are expected. These non-minimal scenarios are of particular interest in those cases where constraints on the VL fermion masses are stringent. As we have demonstrated, decoupling in such cases is severe and strongly depletes the cross-section. Thus, the inclusion of additional generations can potentially open regions of parameter space that otherwise are closed.

In addition to addressing the results reported by ATLAS, the heavy Higgs resonance we have put forward leads to several other *remarkable predictions*. First of all, the to-some-extent small mass splitting between the heavy CP-even and CP-odd states leads necessarily to triboson signatures, $W^\pm W^\mp Z$ and $Z Z Z$ [43]. Secondly, charged Higgs single production, being Cabibbo suppressed and driven by SM couplings is negligible. Thus, it is not possible to generate an excess in the $W^\pm Z$ channel in this setup. Finally, sufficiently large H cross-sections require vector-like fermion masses below ~ 3 TeV, hence being potentially producible at LHC.

We conclude by emphasizing that if the ~ 2 diboson resonance were to be confirmed, LHC data should as well tell us soon whether the mechanism we have pointed out here is responsible for such observation: the diboson signal should be accompanied by a CP-odd Higgs whose mass should not exceed ~ 2.3 TeV, TeV-colored fermions should be copiously produced, no statistically significant diboson events in the $W^\pm Z$ channel should be observed, while there should be a signal in the triboson channels ($W^\pm W^\mp Z, Z Z Z$). Therefore, the model we have discussed here will be soon subject to deep experimental scrutiny.

ACKNOWLEDGEMENTS

We would like to thank Frank Deppisch, Martin Hirsch, Suchita Kulkarni and Werner Porod for useful conversations. DAS would like to acknowledge financial support from the Belgian FNRS agency through a “Chargé de Recherche” contract.

-
- [1] ATLAS, G. Aad *et al.*, (2015), arXiv:1506.00962.
- [2] CMS, V. Khachatryan *et al.*, JHEP **08**, 173 (2014), arXiv:1405.1994.
- [3] CMS, V. Khachatryan *et al.*, JHEP **08**, 174 (2014), arXiv:1405.3447.
- [4] B. C. Allanach, B. Gripaios, and D. Sutherland, Phys. Rev. **D92**, 055003 (2015), arXiv:1507.01638.
- [5] D. Gonçalves, F. Krauss, and M. Spannowsky, Phys. Rev. **D92**, 053010 (2015), arXiv:1508.04162.
- [6] L. Bian, D. Liu, J. Shu, and Y. Zhang, (2015), arXiv:1509.02787.
- [7] D. Kim, K. Kong, H. M. Lee, and S. C. Park, (2015), arXiv:1507.06312.
- [8] S. P. Liew and S. Shirai, (2015), arXiv:1507.08273.
- [9] T. Bandyopadhyay, B. Brahmachari, and A. Raychaudhuri, (2015), arXiv:1509.03232.
- [10] R. L. Awasthi, P. S. B. Dev, and M. Mitra, (2015), arXiv:1509.05387.
- [11] H. S. Fukano, M. Kurachi, S. Matsuzaki, K. Terashi, and K. Yamawaki, Phys. Lett. **B750**, 259 (2015), arXiv:1506.03751.
- [12] J. Hisano, N. Nagata, and Y. Omura, Phys. Rev. **D92**, 055001 (2015), arXiv:1506.03931.
- [13] D. B. Franzosi, M. T. Frandsen, and F. Sannino, (2015), arXiv:1506.04392.
- [14] K. Cheung, W.-Y. Keung, P.-Y. Tseng, and T.-C. Yuan, (2015), arXiv:1506.06064.
- [15] B. A. Dobrescu and Z. Liu, (2015), arXiv:1506.06736.
- [16] A. Alves, A. Berlin, S. Profumo, and F. S. Queiroz, (2015), arXiv:1506.06767.
- [17] Y. Gao, T. Ghosh, K. Sinha, and J.-H. Yu, Phys. Rev. **D92**, 055030 (2015), arXiv:1506.07511.
- [18] A. Thamm, R. Torre, and A. Wulzer, (2015), arXiv:1506.08688.
- [19] J. Brehmer, J. Hewett, J. Kopp, T. Rizzo, and J. Tattersall, (2015), arXiv:1507.00013.
- [20] Q.-H. Cao, B. Yan, and D.-M. Zhang, (2015), arXiv:1507.00268.
- [21] G. Cacciapaglia and M. T. Frandsen, Phys. Rev. **D92**, 055035 (2015), arXiv:1507.00900.
- [22] T. Abe, R. Nagai, S. Okawa, and M. Tanabashi, Phys. Rev. **D92**, 055016 (2015), arXiv:1507.01185.
- [23] J. Heeck and S. Patra, Phys. Rev. Lett. **115**, 121804 (2015), arXiv:1507.01584.
- [24] T. Abe, T. Kitahara, and M. M. Nojiri, (2015), arXiv:1507.01681.
- [25] A. Carmona, A. Delgado, M. Quirós, and J. Santiago, JHEP **09**, 186 (2015), arXiv:1507.01914.
- [26] B. A. Dobrescu and Z. Liu, (2015), arXiv:1507.01923.
- [27] H. S. Fukano, S. Matsuzaki, and K. Yamawaki, (2015), arXiv:1507.03428.
- [28] M. E. Krauss and W. Porod, Phys. Rev. **D92**, 055019 (2015), arXiv:1507.04349.
- [29] L. A. Anchordoqui *et al.*, Phys. Lett. **B749**, 484 (2015), arXiv:1507.05299.
- [30] L. Bian, D. Liu, and J. Shu, (2015), arXiv:1507.06018.
- [31] K. Lane and L. Prichett, (2015), arXiv:1507.07102.
- [32] M. Low, A. Tesi, and L.-T. Wang, (2015), arXiv:1507.07557.
- [33] H. Terazawa and M. Yasue, (2015), arXiv:1508.00172.
- [34] P. Arnan, D. Espriu, and F. Mescia, (2015), arXiv:1508.00174.
- [35] C. Niehoff, P. Stangl, and D. M. Straub, (2015), arXiv:1508.00569.
- [36] P. S. B. Dev and R. N. Mohapatra, (2015), arXiv:1508.02277.
- [37] A. Dobado, F.-K. Guo, and F. J. Llanes-Estrada, (2015), arXiv:1508.03544.
- [38] F. F. Deppisch *et al.*, (2015), arXiv:1508.05940.
- [39] U. Aydemir, D. Minic, C. Sun, and T. Takeuchi, (2015), arXiv:1509.01606.
- [40] A. Dobado, R. L. Delgado, and F. J. Llanes-Estrada, (2015), arXiv:1509.04725.
- [41] T. Li, J. A. Maxin, V. E. Mayes, and D. V. Nanopoulos, (2015), arXiv:1509.06821.
- [42] V. Sanz, (2015), arXiv:1507.03553.
- [43] J. A. Aguilar-Saavedra, (2015), arXiv:1506.06739.
- [44] C.-W. Chiang, H. Fukuda, K. Harigaya, M. Ibe, and T. T. Yanagida, (2015), arXiv:1507.02483.
- [45] G. Cacciapaglia, A. Deandrea, and M. Hashimoto, (2015), arXiv:1507.03098.
- [46] C.-H. Chen and T. Nomura, Phys. Lett. **B749**, 464 (2015), arXiv:1507.04431.
- [47] Y. Omura, K. Tobe, and K. Tsumura, Phys. Rev. **D92**, 055015 (2015), arXiv:1507.05028.
- [48] W. Chao, (2015), arXiv:1507.05310.
- [49] C. Petersson and R. Torre, (2015), arXiv:1508.05632.
- [50] S. Zheng, (2015), arXiv:1508.06014.
- [51] S. Fichtel and G. von Gersdorff, (2015), arXiv:1508.04814.
- [52] R. Dermisek, E. Lunghi, and S. Shin, (2015), arXiv:1509.04292.
- [53] C.-H. Chen and T. Nomura, (2015), arXiv:1509.02039.
- [54] V. Ilisie and A. Pich, Phys. Rev. **D86**, 033001 (2012), arXiv:1202.3420.
- [55] J. F. Gunion and H. E. Haber, Phys. Rev. **D67**, 075019 (2003), arXiv:hep-ph/0207010.
- [56] G. C. Branco *et al.*, Phys. Rept. **516**, 1 (2012), arXiv:1106.0034.
- [57] Particle Data Group, K. A. Olive *et al.*, Chin. Phys. **C38**, 090001 (2014).
- [58] J. A. Aguilar-Saavedra, R. Benbrik, S. Heinemeyer, and M. Pérez-Victoria, Phys. Rev. **D88**, 094010 (2013), arXiv:1306.0572.
- [59] J. A. Aguilar-Saavedra, Phys. Rev. **D67**, 035003 (2003), arXiv:hep-ph/0210112, [Erratum: Phys. Rev. **D69**, 099901 (2004)].
- [60] G. Barenboim, F. J. Botella, and O. Vives, Nucl. Phys. **B613**, 285 (2001), arXiv:hep-ph/0105306.
- [61] D. A. Camargo, (2015), arXiv:1509.04263.
- [62] J. Kumar, A. Rajaraman, and B. Thomas, Phys. Rev. **D84**, 115005 (2011), arXiv:1108.3333.
- [63] S. A. R. Ellis, R. M. Godbole, S. Gopalakrishna, and J. D. Wells, JHEP **09**, 130 (2014), arXiv:1404.4398.
- [64] D. Carmi, A. Falkowski, E. Kuflik, T. Volansky, and J. Zupan, JHEP **10**, 196 (2012), arXiv:1207.1718.
- [65] O. Eberhardt, U. Nierste, and M. Wiebusch, JHEP **07**, 118 (2013), arXiv:1305.1649.

⁸ Note that even using the most stringent bounds they can yield a consistent signal in the case $n_{VL} > 1$.

- [66] A. Barroso, P. M. Ferreira, R. Santos, M. Sher, and J. P. Silva, 2HDM at the LHC - the story so far, in *1st Toyama International Workshop on Higgs as a Probe of New Physics 2013 (HPNP2013) Toyama, Japan, February 13-16, 2013*, 2013, arXiv:1304.5225.
- [67] ATLAS, G. Aad *et al.*, Phys. Lett. **B716**, 1 (2013), arXiv:1207.7214.
- [68] CMS, S. Chatrchyan *et al.*, Phys. Lett. **B716**, 30 (2013), arXiv:1207.7235.
- [69] P. M. Ferreira *et al.*, The CP-conserving 2HDM after the 8 TeV run, in *Proceedings, 22nd International Workshop on Deep-Inelastic Scattering and Related Subjects (DIS 2014)*, 2014, arXiv:1407.4396.
- [70] A. Djouadi, Phys. Rept. **457**, 1 (2008), arXiv:hep-ph/0503172.
- [71] W. E. Caswell, Phys. Rev. Lett. **33**, 244 (1974).
- [72] D. R. T. Jones, Nucl. Phys. **B75**, 531 (1974).
- [73] G. D. Mack, J. F. Beacom, and G. Bertone, Phys. Rev. **D76**, 043523 (2007), arXiv:0705.4298.
- [74] ATLAS, G. Aad *et al.*, Eur. Phys. J. **C75**, 407 (2015), arXiv:1506.05332.
- [75] ATLAS, G. Aad *et al.*, Phys. Rev. **D91**, 112016 (2015), arXiv:1502.05686.
- [76] Y. Okada and L. Panizzi, Adv. High Energy Phys. **2013**, 364936 (2013), arXiv:1207.5607.
- [77] CMS, S. Chatrchyan *et al.*, Phys. Rev. **D86**, 112003 (2012), arXiv:1209.1062.
- [78] A. D. Martin, W. J. Stirling, R. S. Thorne, and G. Watt, Eur. Phys. J. **C63**, 189 (2009), arXiv:0901.0002.
- [79] B. A. Dobrescu, G. D. Kribs, and A. Martin, Phys. Rev. **D85**, 074031 (2012), arXiv:1112.2208.